13º WETE
16, 17 e 18 de novembro de 2022
13º Workshop em Engenharia e Tecnologia Espaciais

Deposition and characterization of AlGaN films produced using reactive magnetron sputtering

Isabela Machado Horta [1*], André Luis de Jesus Pereira [1], Douglas Marcel Gonçalves Leite [1]

[1]Instituto Tecnológico da Aeronáutica, São José dos Campos, SP, Brasil – Departamento de Engenharia Aeronáutica e Mecânica

ihorta@ita.br

Abstract. This work reports the deposition and characterization of sputtered $Al_xGa_{1-x}N$ films on Si (100) substrates with different compositions. The main objective is to study the effect of the composition on the structural quality and c-axis orientation of the films, which is desirable for application in surface acoustic wave sensors. The samples were produced using different powers applied on individual Al and Ga targets in order to vary the composition, and the Al molar fraction was in the range $0 \leq x \leq 0.47$. The other deposition parameters were kept fixed. Samples were characterized using energy dispersive spectroscopy, optical profilometry and X-ray diffraction. Results showed a strong correlation between the films properties and the composition, but also an influence of the thickness of the samples. All samples showed wurtzite structure and the c-axis orientation increased with the Al molar fraction.

Keywords: AlGaN; Sputtering; Characterization; Films; Semiconductor.

1. Introduction

III-nitrides thin films such as GaN and AlGaN are highly attractive materials for application in sensors, transistors, light-emitting diodes (LEDs), and other optoelectronic devices. These films are usually produced using techniques as metalorganic chemical vapor deposition (MOCVD) or metalorganic vapor phase epitaxy (MOVPE), and molecular beam epitaxy (MBE), which are expensive and require high temperatures (JUNAID et al., 2018; LU et al., 2004; NI et al., 2015). However, magnetron sputtering deposition technique is a well stablished process that has shown to efficiently produce high quality thin films of III-nitrides, like AlN and GaN (OLIVEIRA, FOLLI, *et al.*, 2022, SCHIABER, LEITE, *et al.*, 2013, SHIGEKAWA, NISHIMURA, *et al.*, 2007, SIGNORE, BELLINI, *et al.*, 2013). This technique has a lower production cost, compatibility with several materials and sizes, and can operate at low temperatures.

Particularly, GaN and AlGaN thin films and heterostructures on silicon substrates are attractive for surface acoustic wave (SAW) devices due to its piezoelectric properties and the possibility to create a charge carrier rich interface, which, besides increasing the acoustic wave velocity, may increase the devices sensitivity (SHIGEKAWA, NISHIMURA, *et al.*,

2007). Although AlN thin films have been produced with reactive magnetron sputtering deposition with high quality and for SAW devices applications (RODRÍGUEZ-MADRID, IRIARTE, *et al.*, 2012, TIGLI, ZAGHLOUL, 2010), there is a gap of reports on AlGaN thin films using this deposition technique.

Moreover, SAW sensors are used in a wide range of applications, from military, radar and satellites to communication and mobile phones (AMBACHER, 1998, GIANNAZZO, GRECO, *et al.*, 2019). Piezoelectric materials, with high surface acoustic wave velocity, smooth surface, high electromechanical coupling factor and small transition loss are very attractive for application in those SAW devices and sensors, which makes thin films of group-III nitrides interesting for such application (AMBACHER, 1998).

The main objective of this research is to produce and characterize the sputtered $Al_xGa_{1-x}N$ thin films to correlate its structural properties and characteristics such as lattice parameters, strains, c-axis orientation and crystallite size with the film's composition.

2. Methodology

All depositions were carried in a sputtering system dedicated to III-nitrides on the Plasma and Processes Laboratory from Aeronautics Institute of Technology (ITA). The deposition chamber (KJ Lesker, P/N SP1800S-316LN-EP) is equipped with a mechanical vacuum pump and a turbo molecular pump system. The Ga source is a liquid 4-inch target (99.999% purity) and is located on the inferior part of the chamber facing the center. The 1-inch Al target (99.999% purity) is located on the lateral, radially directed to the center of the chamber. The power supply is a DC (controlled by either power or current) supply, which is connected to the Al target, and a RF power supply (13.56 MHz) which is connected to the Ga target. Argon and nitrogen are independently supplemented to the system, precisely controlled by mass flows. The substrate holder allows the deposition of 6 simultaneous samples with 15 mm of diameter.

The AlGaN samples were produced varying the Al power and the Ga power, while keeping all other deposition parameters fixed, which are shown on Table 1. Such decision was made in order to study the composition effect on the different samples' characteristics. Prior to deposition, the Si substrates were cleaned using a typical RCA procedure, and etched in a HF solution (20%) to remove oxides from the surface.

Table 1: Fixed deposition parameters used for all AlGaN samples.

Deposition parameter	Fixed value
Temperature (ºC)	550
Ar:N2 ratio	7:14
Pressure (Torr)	5x10-3
Substrate rotation (rpm)	6
Ga target-to-substrate distance (mm)	90
Deposition time (min)	120

The Ga target power were selected as 30, 60 and 90 W, and the Al target power were 50, 75 and 100 W. Besides, a sample was produced using only the Ga target at 60 W to produce a film with 0% Al (GaN). In total, 10 samples with different composition were produced, ranging from 0 to 0.47 of aluminum molar fraction.

The samples were characterized using energy dispersive X-ray spectroscopy (EDS), profilometry, and X-ray diffractometry (XRD).

Profilometry analyses were made to initially determine film thickness. The measurements were made using an optical profilometer (NanoCalc-VIS by Ocean Optics). For each sample, the measurements were taken simulating both a GaN and an AlN layer on top of the Si substrate, and the thickness was determined by the mean of both analyses.

Energy dispersive spectroscopy (Oxford X-act instrument) was performed on a Vega 3 (Tescan) scanning electron microscope to determine the Al content on the $Al_xGa_{1-x}N$ samples. To assure the reliability of the measurements, the analyses were made on three different points of each sample and the Al molar fraction was determined using an arithmetic mean.

The XRD characterization study was done on a PANalytical Empyrean equipment. The measurements were performed using θ-2θ configuration. All measurements were made using a ½ ° anti-scatter slit and a 10 mm mask for the incident beam, and a 15.4 mm anti-scatter slit for the diffracted beam, under 40 kV and 40 mA for the generator's tension and current, respectively. The scan speed was 0.01 °/s. The angle range was 30 to 65° in order to avoid the monocrystalline Si peaks and obtain the expected peaks for the AlGaN. The analyses were carried out to determine the crystalline structure, the lattice parameters, crystallite size and strains on the films.

3. Results and Discussion

The composition of the films was obtained using EDS, and the results are shown on Table 2. The effects of the power applied to the targets on the composition of the samples are described on Figure 1, which shows the correlation between the measured Al content and the ratio of the Al target power with the sum of the power applied to both targets, corrected with the surface area of the targets (4 inches for the Ga and 1 inch for the Al).

A direct relation between composition and the relative power can be noticed, meaning that, as the relative power applied to the Al increases, the Al composition also increases. However, the influence of the targets can still be seen, as samples with the same ratio were able to show very similar (0.07 of Al fraction) or very different (0.12 and 0.24) compositions.

The thickness of the samples is also displayed on Table 2, which shows that the power applied to the Ga target was the main influence on the thickness and deposition rate, followed by the power applied to the Al target. Once all samples used the same deposition time (120 min), the samples' thicknesses are directly related to their deposition rates, which are influenced by the targets surface area and composition.

Table 2: Al composition for the AlGaN samples for the different applied powers.

Al target power (W)	Ga target power (W)	Al content	Thickness (nm)
0	60	0	253 ± 51
50	90	0.04	678 ± 69
75	90	0.07	805 ± 79
50	60	0.07	352 ± 36
100	90	0.09	770 ± 77
75	60	0.11	398 ± 41
100	60	0.13	407 ± 42
50	30	0.24	116 ± 14
75	30	0.38	166 ± 18
100	30	0.47	193 ± 20

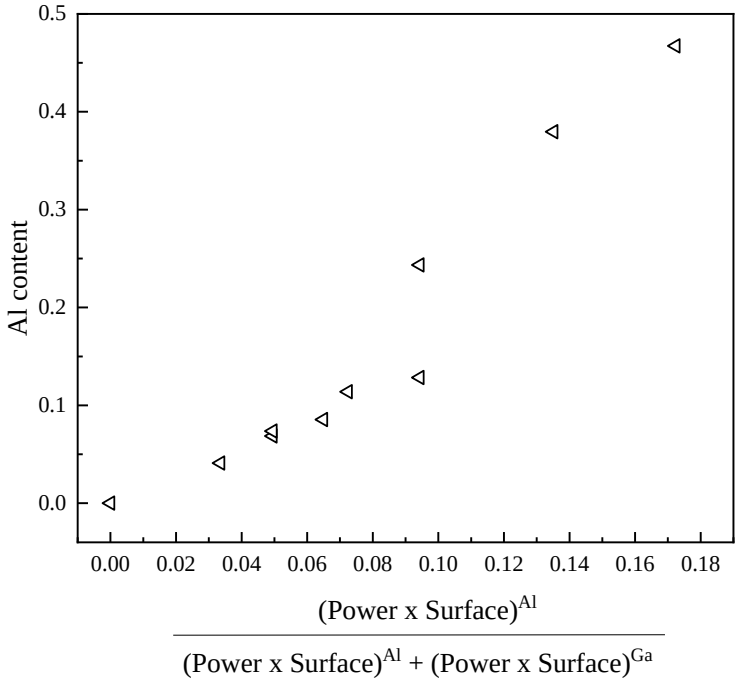

Figure 1: Al content in relation to the relative power applied to the Al target.

The diffractograms for the AlGaN samples are shown on Figure 2 (a). A peak related to the (0002) plane can be seen on all samples, and its position shifts according to the increase in Al molar fraction, as expected (MORAM, VICKERS, 2009), which can be seen more clearly on Figure 2 (b). A second peak related to the (10$\underline{1}$1) plane (expected at 36.86° for GaN) appears for some samples with low Al content (0.08 or less). The relative intensity for the (0002) is a good indicative of this preferential orientation, and is seen related to rocking

curve analyses in other studies (CHANG, YANG, *et al.*, 2014). A general increase on the (0002) intensity occurs as Al molar fraction increases on the samples. The increase in Al fraction could induce a more c-oriented growth on the samples, leading to what is observed on the diffractograms, related to what is expected from AlN grown using sputtering deposition (CHANG, YANG, *et al.*, 2014). The samples GaN, $Al_{0.07}Ga_{0.93}N^{b}$, $Al_{0.11}Ga_{0.89}N$ and $Al_{0.13}Ga_{0.87}N$, which were produced using 60 W on the Ga target supply, showed a lower quality when compared to the samples with less Al molar fraction ($Al_{0.04}Ga_{0.96}N$, $Al_{0.07}Ga_{0.93}N^{a}$ and $Al_{0.09}Ga_{0.91}N$). However, these samples have higher thicknesses, being produced using 90 W on the Ga target. In this sense, the general crystalline quality and the c-axis orientation could be linked to either the sample's composition or the thickness, according to the growth mechanism of the films (HWANG, CHEN, *et al.*, 2002).

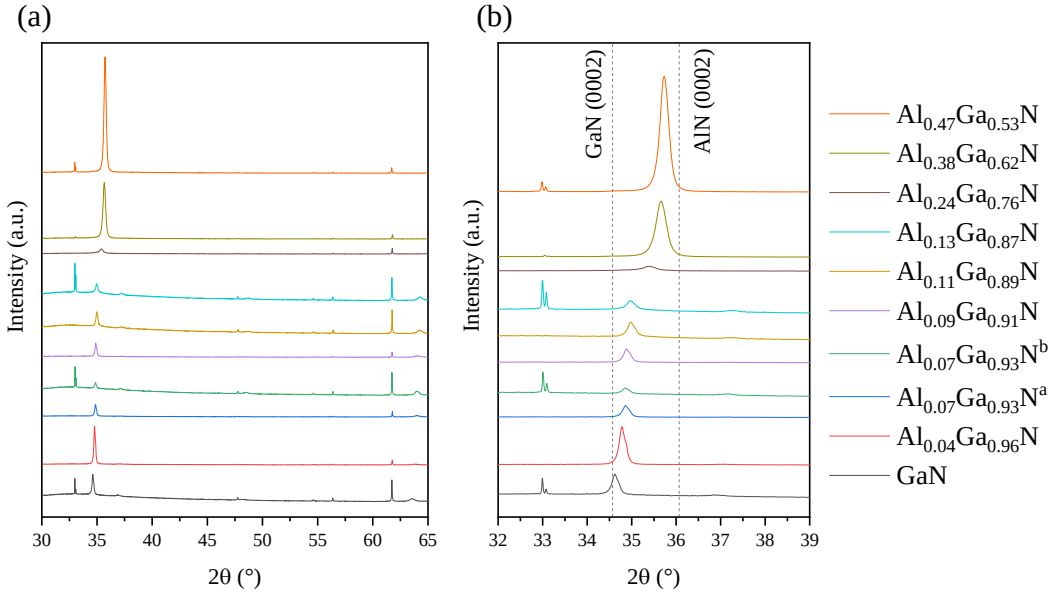

Figure 2: (a) Diffractograms of the AlGaN samples and (b) detailed region for the (0002) peak. Dashed lines indicate the expected position for the (0002) peak for GaN and AlN. [a]90 W on the Ga target and 75 W on the Al target. [b]60 W on the Ga target and 50 W on the Al target.

The lattice parameters *a* and *c* are shown on Figure 3 and the values parameters for unstrained GaN and AlN are marked as dashed lines respectively (SCHULZ, THIEMANN, 1977). For samples with more than 0.12 of Al, the lack of peaks related to planes other than the (0002) prevented the calculation of the lattice parameter *a*. A decrease on *a* and *c* can be seen as Al content increases, which is the expected behavior. Some studies show this to occur linearly, but this behavior is somewhat disturbed by the strains and defects on the films (BERNARDINI, FIORENTINI, 2001, KORAKAKIS, NG, *et al.*, 1996, NOVIKOV, STADDON, *et al.*, 2015).

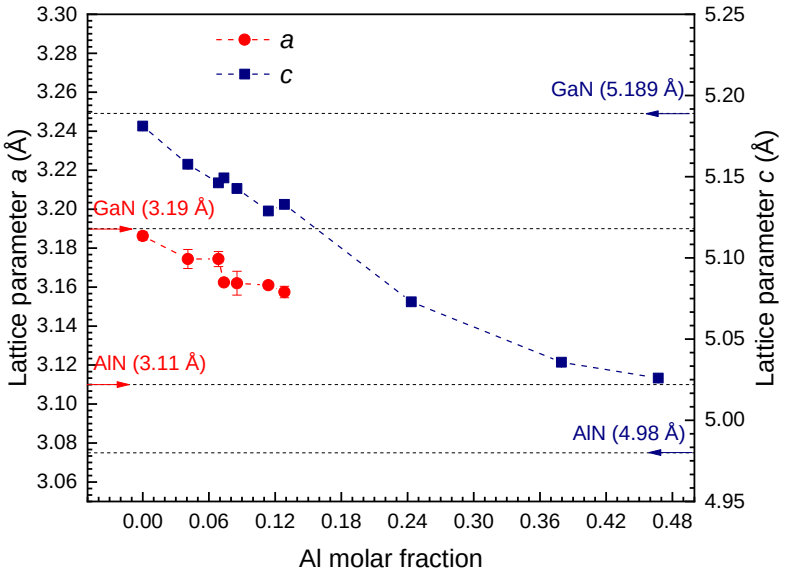

Figure 3: Lattice parameters *a* and *c* for AlGaN samples on Si (100) substrates. The expected values for the unstrained GaN and AlN lattice parameters are indicated.

The crystallite size on the c-axis direction, related to the full width at half maximum (FWHM) of the (0002) peak, can be an indicative of the film general quality, and it is shown on Table 3. As Al increases on the composition, there is a general decrease of crystallite size. This behavior could be compared to another studies, where the FWHM of AlGaN samples deposited on sapphire substrates with AlN buffer layer seemed to increase with Al content (FENG, SARAVADE, *et al.*, 2019, WANG, ZHANG, *et al.*, 2017).

Table 3: Values of crystallite size, in-plane (ε_{xx}) and out-of-plane (ε_{zz}) strains for the AlGaN films.

Al composition	Crystallite size (Å)	ε_{xx} (%)	ε_{zz} (%)
0	452.3 ± 4.5	-0.12 ± 0.07	-0.15 ± 0.01
0.04	459.0 ± 2.7	-0.39 ± 0.15	-0.45 ± 0.01
0.07	436.8 ± 2.6	-0.32 ± 0.12	-0.55 ± 0.01
0.07	444.9 ± 17.6	-0.68 ± 0.04	-0.47 ± 0.01
0.09	441.3 ± 2.6	-0.67 ± 0.19	-0.55 ± 0.01
0.11	409.5 ± 3.2	-0.63 ± 0.05	-0.70 ± 0.01
0.13	359.5 ± 26.8	-0.70 ± 0.09	-0.56 ± 0.02
0.24	241.2 ± 2.8	-	-1.25 ± 0.01
0.38	298.4 ± 0.9	-	-1.42 ± 0.01
0.47	355.7 ± 1.1	-	-1.25 ± 0.01

It is important to notice, when analyzing the crystallite size for the samples, that the high Al-content ones all have small thicknesses (less than 200 nm). This could influence the values of FWHM observed leading to believe that their low quality is related to the composition. However, some studies have shown a relation between the measured FWHM and the thickness of thin films (DUQUENNE, DJOUADI, *et al.*, 2008, LEE, JOO, *et al.*, 2014, SUN, ZHANG, *et al.*, 2016). Therefore, the values of crystallite size must be carefully looked into when judging the overall quality of the sample.

The lattice parameters show a divergence from the expected unstrained values, which indicates strains on the films. Those in-plane and out-of-plane strains were calculated based on lattice parameters and are shown on Table 3. The values become higher (more compressive) as Al increases in composition, which is similar to what was observed on references (FENG, SARAVADE, *et al.*, 2019).

4. Conclusion

The deposition of AlGaN thin films using magnetron sputtering showed that the Al content had a significant influence on the film's structural properties. Overall, the increase in Al content led to more c-axis oriented samples. It also led to a shift on the (0002) peak position and variation of the lattice parameters *a* and *c*. The deviation of the peak position from the unstrained expected one was increased the composition. This behavior was associated with strains on the structure, which increases with Al molar fraction.

The thickness of the samples seems to highly influence the crystallite size obtained from the FWHM of the (0002) peak, and could also be influencing the calculated strains. Without considering this property, the samples with low Al molar fraction produced using the higher power on the Ga target, i.e., samples $Al_{0.04}Ga_{0.96}N$, $Al_{0.07}Ga_{0.93}N^{a}$ and $Al_{0.09}Ga_{0.91}N$, are the ones with a better relation of low strains and large crystallites. For the more pronounced c-axis orientation, the samples with higher Al content (0.24, 0.38 and 0.45 Al) show better results and more relatively intense (0002) peaks.

Acknowledgements: *The authors thank CAPES for the funding of this doctorate project (Grant 88887.509345/2020-00), and the financial support of Fapesp (Grants 2015/06241-5, 2011/50773-0) and CNPq (Grants 428591/2018- 3, 159754/2018-6 and 307199/2018-5). The authors also thank the Plasma and Processes Laboratory from Aeronautics Institute of Technology (LPP-ITA) for the infrastructure and support.*

References

AMBACHER, O. "Growth and applications of group III-nitrides", **Journal of Physics D: Applied Physics**, v. 31, n. 20, p. 2653–2710, 1998. DOI: 10.1088/0022-3727/31/20/001. .

BERNARDINI, F., FIORENTINI, V. "Nonlinear macroscopic polarization in III-V nitride alloys", **Physical Review B**, v. 64, n. 8, p. 085207, 8 ago. 2001. DOI: 10.1103/PhysRevB.64.085207. Disponível em: https://link.aps.org/doi/10.1103/PhysRevB.64.085207.

CHANG, C.-T., YANG, Y.-C., LEE, J.-W., *et al.* "The influence of deposition parameters on the structure and properties of aluminum nitride coatings deposited by high power impulse magnetron sputtering", **Thin Solid Films**, v. 572, p. 161–168, dez. 2014. DOI: 10.1016/j.tsf.2014.09.007. Disponível em: https://linkinghub.elsevier.com/retrieve/pii/S0040609014008840.

DUQUENNE, C., DJOUADI, M. A., TESSIER, P. Y., *et al.* "Epitaxial growth of aluminum nitride on AlGaN by reactive sputtering at low temperature", **Applied Physics Letters**, v. 93, n. 5, p. 052905, 4 ago. 2008. DOI: 10.1063/1.2967816. Disponível em: http://aip.scitation.org/doi/10.1063/1.2967816.

FENG, Y., SARAVADE, V., CHUNG, T.-F., *et al.* "Strain-stress study of AlxGa1−xN/AlN heterostructures on c-plane sapphire and related optical properties", **Scientific Reports**, v. 9, n. 1, p. 10172, 15 dez. 2019. DOI: 10.1038/s41598-019-46628-4. Disponível em: http://www.nature.com/articles/s41598-019-46628-4.

GIANNAZZO, F., GRECO, G., SCHILIRÒ, E., *et al.* "High-Performance Graphene/AlGaN/GaN Schottky Junctions for Hot Electron Transistors", **ACS Applied Electronic Materials**, v. 1, n. 11, p. 2342–2354, 2019. DOI: 10.1021/acsaelm.9b00530. .

HWANG, B.-H., CHEN, C.-S., LU, H.-Y., *et al.* "Growth mechanism of reactively sputtered aluminum nitride thin films", **Materials Science and Engineering: A**, v. 325, n. 1–2, p. 380–388, fev. 2002. DOI: 10.1016/S0921-5093(01)01477-0. Disponível em: https://linkinghub.elsevier.com/retrieve/pii/S0921509301014770.

KORAKAKIS, D., NG, H. M., MISRA, M., *et al.* "Growth and Doping of AlGaN Alloys by ECR-assisted MBE", **MRS Internet Journal of Nitride Semiconductor Research**, v. 1, p. e10, 13 jun. 1996. DOI: 10.1557/S1092578300001824. Disponível em: https://linkinghub.elsevier.com/retrieve/pii/S0079672718300302.

LEE, S.-M., JOO, Y.-H., KIM, C.-I. "Influences of film thickness and annealing temperature on properties of sol–gel derived ZnO–SnO 2 nanocomposite thin film", **Applied Surface Science**, v. 320, p. 494–501, nov. 2014. DOI: 10.1016/j.apsusc.2014.09.099. Disponível em: https://linkinghub.elsevier.com/retrieve/pii/S016943321402090X.

MORAM, M. A., VICKERS, M. E. "X-ray diffraction of III-nitrides", **Reports on Progress in Physics**, v. 72, n. 3, p. 036502, 1 mar. 2009. DOI: 10.1088/0034-4885/72/3/036502. Disponível em: https://iopscience.iop.org/article/10.1088/0034-4885/72/3/036502.

NOVIKOV, S. V., STADDON, C. R., MARTIN, R. W., *et al.* "Molecular beam epitaxy of free-standing wurtzite Al Ga1−N layers", **Journal of Crystal Growth**, v. 425, p. 125–128, set. 2015. DOI: 10.1016/j.jcrysgro.2015.02.010. Disponível em: https://linkinghub.elsevier.com/retrieve/pii/S0022024815000895.

OLIVEIRA, R. S. de, FOLLI, H. A., STEGEMANN, C., *et al.* "Structural, Morphological, Vibrational and Optical Properties of GaN Films Grown by Reactive Sputtering: The Effect of RF Power at Low Working Pressure Limit", **Materials Research**, v. 25, 2022. DOI: 10.1590/1980-5373-mr-2021-0432. Disponível em: http://www.scielo.br/scielo.php?script=sci_arttext&pid=S1516-

14392022000100240&tlng=en.

RODRÍGUEZ-MADRID, J. G., IRIARTE, G. F., ARAUJO, D., *et al.* "Optimization of AlN thin layers on diamond substrates for high frequency SAW resonators", **Materials Letters**, v. 66, n. 1, p. 339–342, 2012. DOI: 10.1016/j.matlet.2011.09.003. Disponível em: http://dx.doi.org/10.1016/j.matlet.2011.09.003.

SCHIABER, Z. S., LEITE, D. M. G., BORTOLETO, J. R. R., *et al.* "Effects of substrate temperature, substrate orientation, and energetic atomic collisions on the structure of GaN films grown by reactive sputtering", **Journal of Applied Physics**, v. 114, n. 18, 2013. DOI: 10.1063/1.4828873. .

SCHULZ, H., THIEMANN, K. H. "Crystal structure refinement of AlN and GaN", **Solid State Communications**, v. 23, n. 11, p. 815–819, set. 1977. DOI: 10.1016/0038-1098(77)90959-0. Disponível em: https://linkinghub.elsevier.com/retrieve/pii/0038109877909590.

SHIGEKAWA, N., NISHIMURA, K., SUEMITSU, T., *et al.* "SAW Filters Composed of Interdigital Schottky and Ohmic Contacts on AlGaN/GaN Heterostructures", **Electron Device Letters, IEEE**, v. 28, n. 2, p. 90–92, 2007. DOI: 10.1109/LED.2006.889043. .

SIGNORE, M. A., BELLINI, E., TAURINO, A., *et al.* "Structural and morphological evolution of aluminum nitride thin films: Influence of additional energy to the sputtering process", **Journal of Physics and Chemistry of Solids**, v. 74, n. 10, p. 1444–1451, 2013. DOI: 10.1016/j.jpcs.2013.05.003. Disponível em: http://dx.doi.org/10.1016/j.jpcs.2013.05.003.

SUN, M. S., ZHANG, J. C., HUANG, J., *et al.* "AlN thin film grown on different substrates by hydride vapor phase epitaxy", **Journal of Crystal Growth**, v. 436, p. 62–67, fev. 2016. DOI: 10.1016/j.jcrysgro.2015.11.040. Disponível em: https://linkinghub.elsevier.com/retrieve/pii/S0022024815007083.

TIGLI, O., ZAGHLOUL, M. E. "Surface acoustic wave (SAW) biosensors". 2010. **Anais** [...] [S.l: s.n.], 2010. p. 77–80. DOI: 10.1109/MWSCAS.2010.5548565.

WANG, S., ZHANG, X., DAI, Q., *et al.* "An X-ray diffraction and Raman spectroscopy investigation of AlGaN epi-layers with high Al composition", **Optik**, v. 131, p. 201–206, fev. 2017. DOI: 10.1016/j.ijleo.2016.11.079. Disponível em: https://linkinghub.elsevier.com/retrieve/pii/S003040261631405X.